

文章编号: 1000-5862(2015)04-0404-07

# The Hydrogen Generation from Hydrolysis of Ammonia Borane via Zeolitic Imidazolate Frameworks Co-ZIF-9

HUANG Wei ,HU Na ,GUI Tian\* ,ZHANG Fei ,CHEN Xiangshu\*

( Jiangxi Inorganic Membrane Materials Engineering Research Centre ,College of Chemistry and  
Chemical Engineering ,Jiangxi Normal University ,Nanchang Jiangxi 330022 ,China)

**Abstract:** Crystalline zeolite imidazolate framework ZIF-9 has been prepared via solvothermal method and used as an efficient heterogeneous catalyst for the hydrolytic dehydrogenation of ammonia borane( AB) complex to generate a stoichiometric of hydrogen at room temperature. Co-ZIF-9 exhibited much higher catalytic activity than the bare Co nanoparticles( NPs) for hydrogen generation from the hydrolysis of AB ,due to that the porous structure of Co-ZIF-9 play an important role in the catalytic hydrolysis of AB. Additionally ,the activation energy for Co-ZIF-9 was measured to be approximately of  $40.8 \text{ kJ} \cdot \text{mol}^{-1}$  ,being lower than most of reported activation energy values for the same reaction using many different catalysts ,indicating the superior catalytic performance of Co-ZIF-9.

**Key words:** ammonia borane; Co-ZIF-9; solvothermal method; hydrolysis; hydrogen generation

中图分类号: TQ 028.8 文献标志码: A DOI: 10.16357/j.cnki.issn1000-5862.2015.04.14

## 0 Introduction

Hydrogen ,owing to its clean burning nature ,high calorific value ,environmentally benign ,has been considered as one of the new energy carriers for heating , transportation ,mechanical power and electricity generation. The storage and separation of hydrogen are the major problems that must be overcome on the way to a hydrogen-powered society<sup>[1-2]</sup>. In the last few decades , different storage solutions have been developed ,such as metal hydrides<sup>[3]</sup> ,sorbent materials<sup>[4]</sup> and chemical hydride systems<sup>[5]</sup>. Among the various kinds of solid hydrogen storage materials ,ammonia borane (  $\text{NH}_3 \cdot \text{BH}_3$  , AB) has recently been considered as a promising candidate for chemical hydrogen storage application due to its high hydrogen content ,low molecular weight ,and

environmentally friendly nature<sup>[5-9]</sup>. There are several methods for the release of hydrogen from AB ,which can be broadly divided into categories ,namely solid thermolysis and solvolysis ( hydrolysis or methanolysis) . However ,thermal dehydrogenation process requires high temperature and power consumption. In contrast , AB is able to release hydrogen via at room temperature hydrolysis reaction in the presence of a suitable catalyst. Thus ,the catalysts are the predominant factor for the hydrolytic dehydrogenation of AB. So far many metals such as noble metals Rh<sup>[10]</sup> ,Ru<sup>[11-12]</sup> ,Pd<sup>[13]</sup> , Pt<sup>[14]</sup> ,Au<sup>[15]</sup> ,and non-noble metals Fe<sup>[16]</sup> ,Co<sup>[17-18]</sup> , Ni<sup>[19-20]</sup> ,Cu<sup>[21-22]</sup> have been investigated for this reaction ,among which noble metal catalysts provide significant catalytic activities in the hydrolysis of AB. For the practical application of this system ,it is important to develop cost effective catalysts.

收稿日期: 2015-04-09

基金项目: 国家“863 计划”新材料技术领域重大专项( 2012AA03A609) ,国家自然科学基金( 21463012 21103074) 和江西省重大科技创新( 20114ACB01200) 资助项目.

通信作者: 陈祥树( 1966-) ,男 ,江西玉山人 ,教授 ,博士 ,博士生导师 ,主要从事无机膜与非均相催化方面的研究;  
桂 田( 1987-) ,女 ,江西抚州人 ,助教 ,硕士 ,主要从事实验技术和管理研究.

Recently, a new class of porous materials known as metal organic frameworks (MOFs)<sup>[24-26]</sup>, especially, the family of zeolitic imidazolate frameworks (ZIFs), has been currently attracted significant attention<sup>[18-19]</sup>. ZIFs have ordered porous structures, with high specific surface area and chemically flexible frameworks, consisting of inorganic metal ions (eg. Zn, Co, Cu) coordinated with organic imidazole or imidazolate ligands. However, since first discovery of the ZIF sample, research efforts have been mostly aimed in preparing new ZIFs and investigating their applications in gas storage and separation. Actually, using ZIFs as catalysts or catalyst supports have been reported very limited in the literature<sup>[27-28]</sup>.

In this work, for the first time, the crystalline zeolite imidazolate framework Co-ZIF-9 has been used as highly efficient catalyst for hydrogen generation from  $\text{NH}_3\text{BH}_3$  for chemical hydrogen storage. Compared with the Co NPs, the Co-ZIF-9 showed higher performance for the dehydrogenation of  $\text{NH}_3\text{BH}_3$  at convenient temperature for chemical hydrogen storage.

## 1 Experimental

### 1.1 Chemicals

All chemicals were commercially obtained and used without further purification. Ammonia borane ( $\text{NH}_3\text{BH}_3$ , AB, Aldrich, 90%), sodium borohydride ( $\text{NaBH}_4$ , Sigma-Aldrich, 99%), cobalt (II) nitrate hexahydrate ( $\text{Co}(\text{NO}_3)_2 \cdot 6\text{H}_2\text{O}$ , Sinopharm Chemical Reagent Co. Ltd., >99%), benzimidazole (H-PhIM, Sigma-Aldrich, 98%), *N, N'*-dimethylformamide (DMF) were used as received. Ultrapure water with the specific resistance of  $18.3 \text{ M}\Omega \cdot \text{cm}$  was obtained by reversed osmosis followed by ion exchange and filtration.

### 1.2 Instrumentation

Powder X-ray diffraction (XRD) studies were performed on a Rigaku RINT-2200 X-ray diffractometer with a  $\text{Cu}_{K\alpha}$  source (40 kV, 20 mA). The morphologies and sizes of the samples were carried out using cold field emission scanning electron microscope (SEM, SU8020). FTIR spectra were collected at room temperature by using a Thermo Nicolet 870 instrument using

KBr discs in the  $500 \sim 4000 \text{ cm}^{-1}$  region.

### 1.3 Preparation of crystalline zeolite imidazolate framework Co-ZIF-9

The Co-ZIF-9 was synthesized using cobalt nitrate hexahydrate ( $\text{Co}(\text{NO}_3)_2 \cdot 6\text{H}_2\text{O}$ ) and benzimidazole (H-PhIM) by a solvothermal method in DMF according to a literature procedure<sup>[29]</sup>. Briefly, 1.05 g  $\text{Co}(\text{NO}_3)_2 \cdot 6\text{H}_2\text{O}$  and 0.3 g H-PhIM were mixed into 90 mL DMF. After stirring, the transparent solution was transferred into a Teflon autoclave. The autoclave was closed and heated at a rate of  $5 \text{ }^\circ\text{C} \cdot \text{min}^{-1}$  to  $130 \text{ }^\circ\text{C}$  in drying oven and held at this temperature for 48 h, then cooled to room temperature at  $0.4 \text{ }^\circ\text{C} \cdot \text{min}^{-1}$ . After crystallization, the as-prepared purple ZIF-9 crystals were filtered and then washed with DMF three times. Finally, ZIF-9 was conducted with vacuum drying at  $80 \text{ }^\circ\text{C}$  for 10 h to obtain ZIF-9 catalyst.

### 1.4 Preparation of cobalt NPs (Co NPs)

The cobalt NPs were prepared by in situ synthesis method.  $\text{Co}(\text{NO}_3)_2 \cdot 6\text{H}_2\text{O}$  was dissolved in 6 mL of distilled water and kept in a 25 mL two-necked round-bottomed flask. Then 4 mL of aqueous solution containing 55 mg of AB and 10 mg  $\text{NaBH}_4$  were added into the flask with shaking.

### 1.5 Hydrolytic dehydrogenation of AB

In a typical experiment, 15 mg Co-ZIF-9 were dispersed in 6 mL distilled water, and kept in a two-necked round-bottomed flask. A burette filled with water was connected to the reaction flask to measure the volume of hydrogen. The reaction started when 4 mL of aqueous solution containing 55 mg of AB and 10 mg  $\text{NaBH}_4$  were added into the flask with vigorous shaking. The reaction was completed when there was no more gas generation. The reactions were carried out at different temperatures (298, 303, 308, 313 K) under ambient atmosphere.

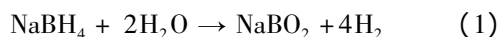
### 1.6 Reusability of Co-ZIF-9 in the hydrolysis of AB

For the durability test of the catalysts, after the first run of hydrogen generation reaction was completed, another equivalent of  $\text{NH}_3\text{BH}_3$  (55 mg) was subsequently added to the reaction system and the released gas was monitored by the gas burette. The reactions were repeated 5 times under ambient atmosphere at room temperature. After cycle test, the catalysts were

separated from the reaction solution by centrifugation, washed with water for three times and dried in vacuum oven at 313 K overnight.

## 2 Result and discussion

Crystalline zeolite imidazolate framework Co-ZIF-9 was prepared using cobalt nitrate hexahydrate and benzimidazole by a solvothermal method and used as cost effective catalyst for the hydrolytic dehydrogenation of ammonia borane( AB) complex to generate a stoichiometric of hydrogen at room temperature. Fig. 1 shows the time course of the hydrogen generation from AB ( $0.16 \text{ mol} \cdot \text{L}^{-1}$ , 10 mL) in the presence of the Co-ZIF-9 and Co catalysts. The catalytic results demonstrated that the reaction rate and the amount of hydrogen evolution significantly depended on the catalysts. As shown in Fig. 1, a stoichiometric amount of hydrogen was evolved in 5.55 min and 9.55 min respectively in the presence of the Co-ZIF-9 and bare Co catalysts. Obviously the as-synthesized Co-ZIF-9 exhibited superior performance in comparison to bare Co NPs for the hydrolytic dehydrogenation of AB at convenient temperature for chemical hydrogen storage. In the present reaction system hydrogen is evolved via the following two reactions:



and

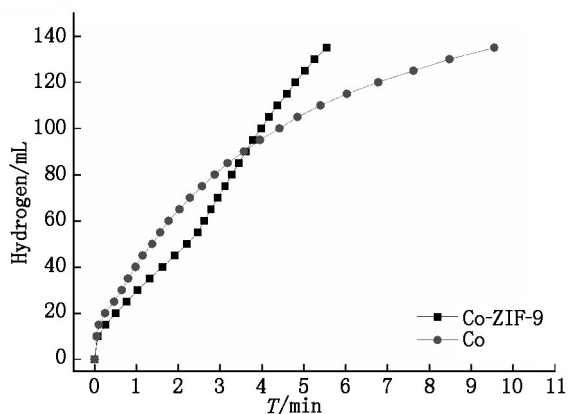


Fig. 1 Hydrogen generation from the hydrolysis of AB ( $0.16 \text{ mol} \cdot \text{L}^{-1}$ , 10 mL) with  $\text{NaBH}_4$  (10 mg) in the presence of (a) Co-ZIF-9, (b) Co at 298 K (catalyst: 15 mg)

Under the present reaction condition, the total amount of hydrogen via reaction (1) and (2) is about

135 mL. Moreover, the turnover frequency (TOF) of the Co-ZIF-9 and bare Co catalysts were measured to be  $9.74$  and  $5.61 \text{ mol H}_2 \cdot \text{mol}^{-1} \text{ Co} \cdot \text{min}^{-1}$ , respectively for the hydrogen generation from the hydrolysis of AB.

Fig. 2 shows the volume of hydrogen generated versus time during the catalytic hydrolysis of AB ( $0.16 \text{ mol} \cdot \text{L}^{-1}$ , 10 mL) solution in the presence of Co-ZIF-9 catalysts with different contents (5, 10, 15, 20, 25, 30 mg) at room temperature. As shown in Fig. 2, when the catalyst content increased the reaction time decreased obviously from 20.2 min to 2.1 min. The hydrogen generation rate is determined from the linear portion of each plot for different cobalt content. The inset of Fig. 3 shows the plot of hydrogen generation rate vs. cobalt contents, both in logarithmic scale. The slope of the obtained line is 1.04, which is closed to 1.00, indicating that the hydrolytic dehydrogenation of AB catalyzed by the Co-ZIF-9 is a first-order reaction with respect to the catalyst concentration.

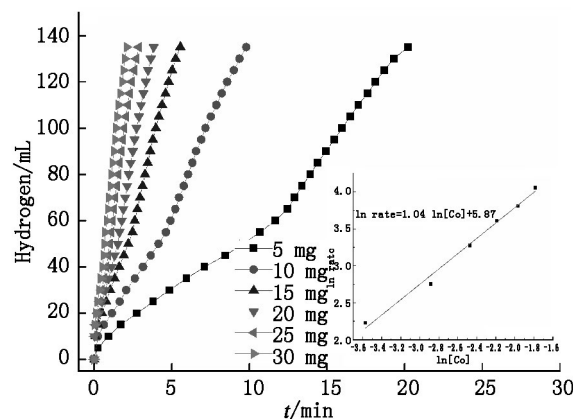


Fig. 2 Hydrogen generation from the hydrolysis of AB ( $0.16 \text{ mol} \cdot \text{L}^{-1}$ , 10 mL) with  $\text{NaBH}_4$  (10 mg) in the presence of Co-ZIF-9 with different contents at 298 K. The inset shows the plot of hydrogen generation rate vs. the contents of Co, both in logarithmic scale

The effect of temperature on the hydrogen generation rate by Co-ZIF-9 was also studied, and a series of experiments were carried out by varying the temperatures. Fig. 3 shows the volume of hydrogen generated versus reaction time in the hydrolysis of AB ( $0.16 \text{ mol} \cdot \text{L}^{-1}$ , 10 mL) catalyzed by Co-ZIF-9 catalysts at various temperatures in the range of 293–308 K. Clearly, with the increase of the reaction temperature, the catalytic activity of the Co-ZIF-9 improves remarkably. The reaction rate constant  $k$  at different

temperatures was estimated from the slope of the linear part of each plot in Fig. 3. The Arrhenius plot of  $\ln k$  versus  $1/T$  for the catalyst is plotted in Fig. 3 (inset), from which the activation energy ( $E_a$ ) for the hydrolytic dehydrogenation of AB is measured to be  $40.8 \text{ kJ} \cdot \text{mol}^{-1}$ , being lower than most the reported activation energy values (Table 1), indicating the superior catalytic performance of the Co-ZIF-9 catalyst.

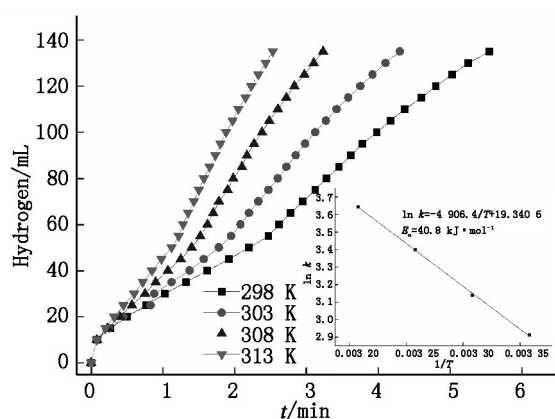


Fig. 3 Hydrogen generation from the hydrolysis of AB ( $0.16 \text{ mol} \cdot \text{L}^{-1}$ ,  $10 \text{ mL}$ ) with  $\text{NaBH}_4$  ( $10 \text{ mg}$ ) in the presence of Co-ZIF-9 ( $15 \text{ mg}$ ) at  $293 \sim 308 \text{ K}$ . The inset shows the Arrhenius plot ( $\ln k$  vs.  $1/T$ )

Table 1 The values of activation energy ( $E_a$ ) for hydrogen generation from aqueous AB at room temperature

Catalyst	$E_a / (\text{kJ} \cdot \text{mol}^{-1})$
Co/ $\gamma$ - $\text{Al}_2\text{O}_3$ [30]	62.0
RuCo/ $\gamma$ - $\text{Al}_2\text{O}_3$ [31]	47.0
Zeolite-confined Cu [22]	$51.8 \pm 1.8$
$\text{Cu}_{0.2} @ \text{Co}_{0.8} / \text{rGo}$ [32]	51.3
CoB/MCM-41 [33]	$51.0 \pm 3.0$
$\text{Cu}_{0.33}\text{Fe}_{0.67}$ [34]	43.2
CoB/SBA-15 [33]	$43.0 \pm 2.0$
Co-ZIF-9	40.8
Ru@ $\text{SiO}_2$ [12]	38.2
Pt/ $\gamma$ - $\text{Al}_2\text{O}_3$ [14]	21.0

The reusability of the Co-ZIF-9 catalyst was tested under ambient atmosphere at room temperature. After complete hydrolysis of AB, the catalyst of Co-ZIF-9 in the reaction solution under ambient conditions and a new AB ( $55 \text{ mg}$ ) was added to the reaction system. Fig. 4 shows the productivity of hydrogen versus reaction time for the generation of hydrogen from an aqueous AB ( $0.16 \text{ mol} \cdot \text{L}^{-1}$ ,  $10 \text{ mL}$ ) solution catalyzed by the Co-ZIF-9. After five runs of the catalytic reaction

for dehydrogenating aqueous AB, the productivity of hydrogen remained almost unchanged, indicating that the Co-ZIF-9 shows good durability/stability for hydrogen generation from the aqueous of AB at room temperature.

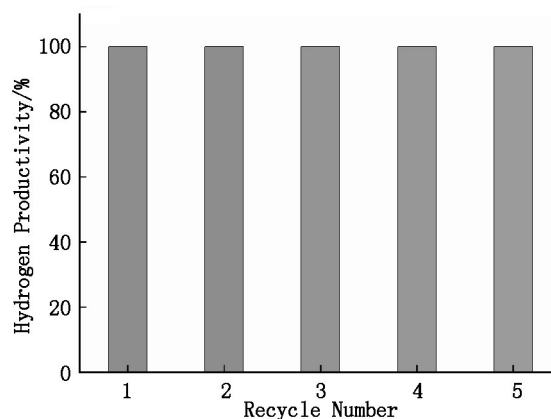


Fig. 4 Hydrogen productivity vs. recycle number for hydrogen generation from the hydrolysis of AB ( $0.16 \text{ mol} \cdot \text{L}^{-1}$ ,  $10 \text{ mL}$ ) in the presence of Co-ZIF-9 ( $15 \text{ mg}$ ) at sequential runs by the addition of equivalent amounts of AB

Powder X-ray diffraction (XRD) was performed on Co-ZIF-9 before and after hydrolysis of AB. As shown in Fig. 5 (a), several sharp peaks were observed on the XRD profile for the fresh Co-ZIF-9. The positions of diffraction peaks indicated that Co-ZIF-9 was highly crystalline material and the recorded pattern corresponds well with the previous reports [26, 29]. Moreover, compared with the fresh and used catalyst revealed that the Co-ZIF-9 could maintain its basic structure and crystallinity after the hydrolytic dehydrogenation of AB.

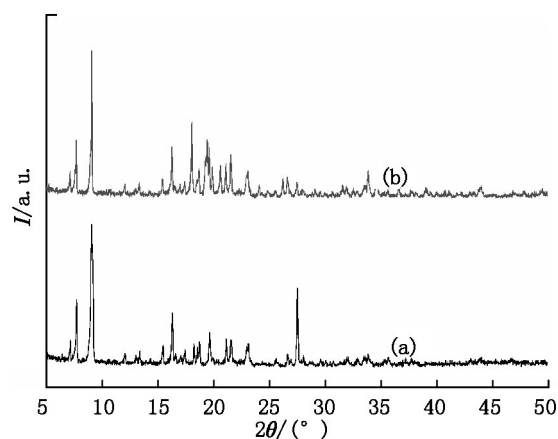


Fig. 5 Powder X-ray diffraction patterns for the (a) reused and (b) fresh of Co-ZIF-9

As expected, the SEM micrograph showed that a crystalline material was achieved (Fig. 6). The morphology of Co-ZIF-9 shows no significant changes be-

fore and after catalytic reaction. Meanwhile, FTIR spectrum showed the same nature, namely, the catalyst of Co-ZIF-9 has not changed much before and after hydrolysis reaction (Fig. 7). These characteristic results

reveal that the catalyst of Co-ZIF-9 has high stability during the hydrogen generation from the hydrolysis of AB.

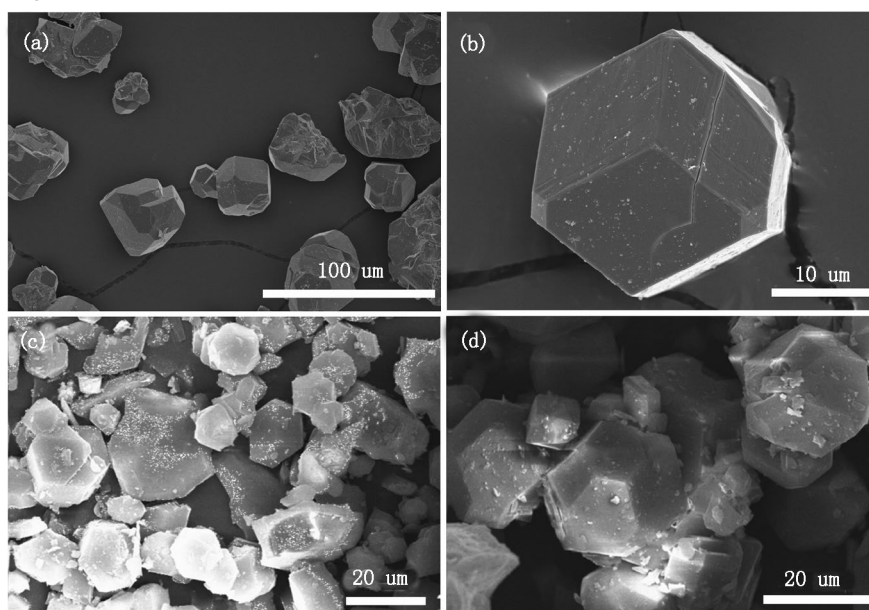


Fig. 6 SEM images of the (a) reused and (b) fresh of Co-ZIF-9

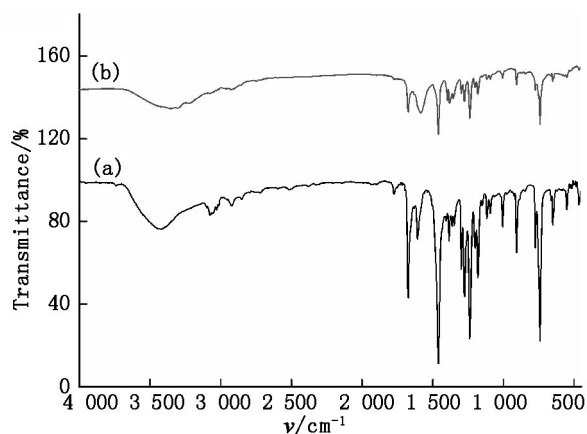


Fig. 7 FT-IR spectra of the (a) reused and (b) fresh of Co-ZIF-9

### 3 Conclusion

In summary, crystalline zeolite imidazolate framework Co-ZIF-9 has been successfully prepared by using the solvothermal method. The catalytic results demonstrated that the Co-ZIF-9 exhibit superior catalytic activity, in comparison to Co NPs, for the dehydrogenation of AB at convenient temperature for chemical hydrogen storage. The hydrolysis activation energy for Co-ZIF-9 was measured to be approximately of  $40.8 \text{ kJ} \cdot \text{mol}^{-1}$ , which is lower than most the reported activation energy

values for the same reaction using many different catalysts except for some noble-metal containing catalysts, indicating the superior catalytic performance of Co-ZIF-9. These results not only present an efficient catalyst for AB hydrolysis, but also provide new insight into the application of Co-ZIF-9 in the field of catalysis.

### 4 References

- [1] Lu Zhanghui, Xu Qiang. Recent progresses in boron- and nitrogen-based chemical hydrogen storage [J]. *Funct Mater Lett* 2012, 5(1): 1230001.
- [2] 张小亮, 卢胜林, 胡志洋, 等. 钕铜合金膜的化学镀制备过程研究 [J]. *江西师范大学学报: 自然科学版* 2010, 34(5): 516-519.
- [3] Graetz J. New approaches to hydrogen storage [J]. *Chem Soc Rev* 2009, 38(1): 73-82.
- [4] Suh M P, Park H J, Prasad T K, et al. Hydrogen storage in metal-organic frameworks [J]. *Chem Rev* 2012, 112(2): 782-835.
- [5] Staubitz A, Robertson A P M, Manners I. Ammonia-borane and related compounds as dihydrogen sources [J]. *Chem Rev* 2010, 110(7): 4079-4124.
- [6] Yadav M, Xu Qiang. Liquid-phase chemical hydrogen storage materials [J]. *Energy Environ Sci*, 2012, 5(12): 9698-9725.

- [7] Jiang Hailong, Xu Qiang. Catalytic hydrolysis of ammonia borane for chemical hydrogen storage [J]. *Catal Today*, 2011, 170(1): 56-63.
- [8] Peng Bo, Chen Jun. Ammonia borane as an efficient and lightweight hydrogen storage medium [J]. *Energy Environ Sci* 2008, 1(4): 479-483.
- [9] Lu Zhanghui, Yao Qilu, Zhang Zhujun, et al. Nanocatalysts for hydrogen generation from ammonia borane and hydrazine borane [J]. *J Nanomaterials* 2014, 2014: 729029.
- [10] Yao Qilu, Lu Zhanghui, Jia Yushuai, et al. In situ facile synthesis of Rh nanoparticles supported on carbon nanotubes as highly active catalysts for H<sub>2</sub> generation from NH<sub>3</sub>BH<sub>3</sub> hydrolysis [J]. *Int J Hydrogen Energy* 2015, 40(5): 2207-2215.
- [11] Akbayrak S, Özkar S. Ruthenium(0) nanoparticles supported on multiwalled carbon nanotube as highly active catalyst for hydrogen generation from ammonia-borane [J]. *ACS Appl Mater Interfaces*, 2012, 4(11): 6302-6310.
- [12] Yao Qilu, Shi Weimei, Feng Gang, et al. Ultrafine Ru nanoparticles embedded in SiO<sub>2</sub> nanospheres: Highly efficient catalysts for hydrolytic dehydrogenation of ammonia borane [J]. *J Power Sources* 2014, 257: 293-299.
- [13] Xi Pinxian, Chen Fengjuan, Xie Guoqiang, et al. Surfactant free RGO/Pd nanocomposites as highly active heterogeneous catalysts for the hydrolytic dehydrogenation of ammonia borane for chemical hydrogen storage [J]. *Nanoscale*, 2012, 4(18): 5597-5601.
- [14] Chandra M, Xu Qiang. Room temperature hydrogen generation from aqueous ammonia-borane using noble metal nano-clusters as highly active catalysts [J]. *J Power Sources* 2007, 168(1): 135-142.
- [15] Lu Zhanghui, Jiang Hailong, Yadav M, et al. Synergistic catalysis of Au-Co@SiO<sub>2</sub> nanospheres in hydrolytic dehydrogenation of ammonia borane for chemical hydrogen storage [J]. *J Mater Chem* 2012, 22(11): 5065-5071.
- [16] Dinc M, Metin Ö, Özkar S. Water soluble polymer stabilized iron(0) nanoclusters: A cost-effective and magnetically recoverable catalyst in hydrogen generation from the hydrolysis of sodium borohydride and ammonia borane [J]. *Catal Today* 2012, 183(1): 10-16.
- [17] Yang Yuwen, Zhang Fei, Wang Hualan, et al. Catalytic hydrolysis of ammonia borane by cobalt nickel nanoparticles supported on reduced graphene oxide for hydrogen generation [J]. *J Nanomater* 2014, 2014: 294350.
- [18] Song Ping, Li Yaoqi, Li Wei, et al. A highly efficient Co(0) catalyst derived from metal-organic framework for the hydrolysis of ammonia borane [J]. *Int J Hydrogen Energy* 2011, 36(1): 10468-10473.
- [19] Li Peizhou, Aranishi K, Xu Qiang. ZIF-8 immobilized nickel nanoparticles: highly effective catalysts for hydrogen generation from hydrolysis of ammonia borane [J]. *Chem Commun* 2012, 48(26): 3173-3175.
- [20] Umegaki T, Yan Junmin, Zhang Xingbo, et al. Hollow Ni-SiO<sub>2</sub> nanosphere-catalyzed hydrolytic dehydrogenation of ammonia borane for chemical hydrogen storage [J]. *J Power Sources* 2009, 191(2): 209-216.
- [21] Yang Yuwen, Lu Zhanghui, Hu Yujuan, et al. Facile in situ synthesis of copper nanoparticles supported on reduced graphene oxide for hydrolytic dehydrogenation of ammonia borane [J]. *RSC Adv* 2014, 4(27): 13749-13752.
- [22] Yao Qilu, Huang Ming, Lu Zhanghui, et al. Methanolysis of ammonia borane by shape-controlled mesoporous copper nanostructures for hydrogen generation [J]. *Dalton Trans*, 2015, 44(3): 1070-1076.
- [23] Yao Qilu, Lu Zhanghui, Zhang Zhujun, et al. One-pot synthesis of core-shell Cu@SiO<sub>2</sub> nanospheres and their catalysis for hydrolytic dehydrogenation of ammonia borane and hydrazine borane [J]. *Sci Rep* 2014, 4: 7597.
- [24] Gu Xiaojun, Lu Zhanghui, Jiang Hailong, et al. Synergistic catalysis of metal-organic framework-immobilized Au-Pd nanoparticles in dehydrogenation of formic acid for chemical hydrogen storage [J]. *J Am Chem Soc*, 2011, 133(31): 11822-11825.
- [25] 乔亚莉, 高楼军, 陈小利, 等. 环状双核钴配合物的合成、晶体结构及其性质 [J]. *江西师范大学学报: 自然科学版* 2012, 36(4): 407-411.
- [26] Zhu Qilong, Li Jun, Xu Qiang. Immobilizing metal nanoparticles to metal-organic frameworks with size and location control for optimizing catalytic performance [J]. *J Am Chem Soc* 2013, 135(28): 10210-10213.
- [27] Battisti A, Taioli S, Garberoglio G. Zeolitic imidazolate frameworks for separation of binary mixtures of CO<sub>2</sub>, CH<sub>4</sub>, N<sub>2</sub> and H<sub>2</sub>: A computer simulation investigation [J]. *Microporous Mesoporous Mater* 2011, 143(1): 46-53.
- [28] Park K S, Ni Zheng, Cote A P, et al. Exceptional chemical and thermal stability of zeolitic imidazolate frameworks [J]. *Proceedings of the National Academy of Sciences of the United States of America*, 2006, 103(27): 10186-10191.
- [29] Li Qiming, Kim H. Hydrogen production from NaBH<sub>4</sub> hydrolysis via Co-ZIF-9 catalyst [J]. *Fuel Process Technol*, 2012, 100: 43-48.
- [30] Xu Qiang, Chandra M. Catalytic activities of non-noble metals for hydrogen generation from aqueous ammonia-borane at room temperature [J]. *J Power Sources* 2006, 163(1): 364-370.
- [31] Rachiero G P, Demirci U B, Miele P. Bimetallic RuCo and RuCu catalysts supported on  $\gamma$ -Al<sub>2</sub>O<sub>3</sub>. A comparative study of their activity in hydrolysis of ammonia-borane

- [J]. *Int J Hydrogen Energy* 2011 36( 12) : 7051-7065.
- [32] Du Yeshuang ,Cao Nan ,Yang Lan ,et al. One-step synthesis of magnetically recyclable rGO supported Cu@ Co core-shell nanoparticles: highly efficient catalysts for hydrolytic dehydrogenation of ammonia borane and methylamine borane [J]. *New J Chem* 2013 37( 10) : 3035-3042.
- [33] Patel N ,Fernandes R ,Gupta S ,et al. Co-B catalyst supported over mesoporous silica for hydrogen production by catalytic hydrolysis of Ammonia Borane: A study on influence of pore structure [J]. *Appl Catal B-Environ* 2013 ,140/141: 125-132.
- [34] Lu Zhanghui ,Li Jinping ,Zhu Aili ,et al. Catalytic hydrolysis of ammonia borane via magnetically recyclable copper iron nanoparticles for chemical hydrogen storage [J]. *Int J Hydrogen Energy* 2013 38( 13) : 5330-5337.

## 沸石咪唑酯骨架结构材料 Co-ZIF-9 催化氨硼烷水解制氢

黄 维 胡 娜 桂 田\* 张 飞 陈祥树\*

(江西师范大学化学化工学院 江西省无机膜材料工程技术研究中心 江西 南昌 330022)

**摘要:** 采用溶剂热方法合成了沸石咪唑酯骨架结构材料 Co-ZIF-9 并将其用于非均相催化氨硼烷水解放氢实验. 结果表明: 配位的 Co-ZIF-9 在室温下能够有效地催化氨硼烷放出氢气, 且其催化活性远高于 Co 纳米粒子, Co-ZIF-9 的多孔结构在催化中起了很大的作用. 另外, Co-ZIF-9 催化水解氨硼烷的活化能约为  $40.8 \text{ kJ mol}^{-1}$ , 低于多数用于该催化实验的其他催化剂, 表明所合成的沸石咪唑酯骨架结构材料 Co-ZIF-9 具有优越的催化性能.

**关键词:** 氨硼烷; 沸石咪唑酯骨架; 溶剂热法; 水解; 制氢

(责任编辑: 刘显亮)

(上接第 388 页)

- 法 [J]. *江西科学* 2009 27( 4) : 569-571.
- [20] 李颖. 基于神经网络的军事目标识别方法研究 [D]. 沈阳: 沈阳理工大学 2005: 10-25.
- [21] 张利华, 马均钊, 勒国庆, 等. 基于 BP 神经网络的仓储烟草霉变预测 [J]. *华东交通大学学报* 2013 30( 3) : 71-75.
- [22] 刘扬. 基于静止气象卫星云图的分类研究 [D]. 青岛: 中国海洋大学 2011: 15-17.
- [23] 郭胜, 徐智勇. 基于数字地球的 3 维云图实现技术 [J]. *首都师范大学学报: 自然科学版* 2013 34( 2) : 70-73.
- [24] 欧阳怡彪. 空间数据挖掘的聚类方法与应用 [D]. 成都: 电子科技大学 2006: 59-76.
- [25] 廖广兰, 史铁林, 刘世元, 等. 基于 GHSOM 网络的故障识别 [J]. *华中科技大学学报: 自然科学版* 2008 36( 7) : 105-107.
- [26] 刘强. 神经网络方法在人脸检测和数据挖掘中的应用 [D]. 成都: 电子科技大学 2005: 55-65.

## The GHSOM Network Cloud Classification Model of Stationary Satellite Infrared Cloud Images at Night

YAN Tingya ,WANG Shan\*

(School of Information Engineering ,East China Jiaotong University ,Nanchang Jiangxi 330013 ,China)

**Abstract:** Aiming at the low accuracy of cloud classification at night ,the features of FY-2E cloud images which include bright temperatures and split window values were extracted and selected based on the method of singular value decomposition. The neural network models of growing hierarchical self-organizing map ( GHSOM) and self-organizing map ( SOM) were built separately to classify cloud images at night ,meanwhile ,contrasting the classified effect of the two network models. The experiments results showed that GHSOM network can improve the distinguishing effect of cloud images at night greatly through hierarchical classified method ,and the average accuracy of cloud classification results is higher than SOM.

**Key words:** growing hierarchical self-organizing map; self-organizing feature map; night cloud image; cloud classification

(责任编辑: 冉小晓)